THE JOURNAL OF PHYSICAL CHEMISTRY Letters

Letter

pubs.acs.org/JPCL

The Mechanism of Iodine Reduction by TiO_2 Electrons and the Kinetics of Recombination in Dye-Sensitized Solar Cells

Caryl E. Richards,[†] Assaf Y. Anderson,[†,‡] Stefano Martiniani,[†] ChunHung Law,[†] and Brian C. O'Regan*[,†]

[†]Department of Chemistry, Imperial College London, Imperial College Road, London, SW7 2AZ, U.K.

[‡]Center for Nanotechnology & Advanced Materials, Bar-Ilan University, Ramat-Gan, Israel 52900

Supporting Information

ABSTRACT: Electron transfer from TiO_2 to iodine/iodide electrolytes proceeds via reduction of either I_3^- or uncomplexed I_2 (free iodine), but which route predominates has not previously been determined. By measurement of the electron lifetime while independently varying free iodine or I_3^- concentrations, we find the lifetime is correlated with free-iodine concentration and independent of I_3^- concentration. This trend supports the hypothesis that electron recombination to the electrolyte occurs predominantly by iodine reduction rather than reduction of triiodide.

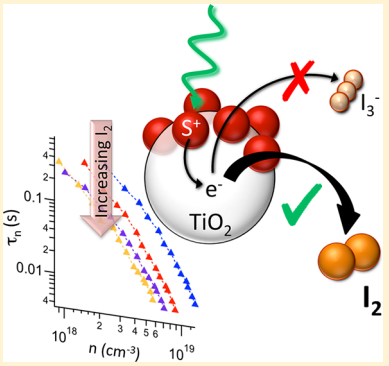

SECTION: Kinetics and Dynamics

Voltage in dye-sensitized solar cells (DSSCs) is limited in part by recombination due to electron transfer from the TiO_2 layer to the oxidized form of the electrolyte. Despite advances with other electrolytes, iodide/triiodide (I^-/I_3^-) remains the redox couple of choice for DSSCs, and a wealth of literature addresses its many facets of recombination.[1−6] Nevertheless, no work to date has definitively identified whether the first step in recombination involves the reduction of iodine or triiodide.

In this Letter, we study this step in the recombination reaction by independently varying the free iodine and triiodide concentration in the electrolyte. Five sets of cells were measured with three different dyes and two different solvents to ensure generality. By correlating the recombination kinetics with the different acceptor concentrations, we conclude that the majority of recombination occurs by direct reduction of iodine, even though it is present at far smaller concentrations than triiodide. This conclusion has implications for the optimization of electrolytes, the interpretation of temperature-dependent studies, and modeling of DSSCs.

EXPERIMENTAL METHODS

Film and Device Fabrication. Glass/glass sandwich-type DSSCs were fabricated in the usual way. Full details of cell preparation have been described previously,[7] but a brief outline of the major steps will be given here. The porous, nanocrystalline films of TiO_2 (crystal size ∼20 nm diameter supplied by Dyesol) were doctor bladed onto a transparent conductive fluorine-doped tin oxide (FTO) substrate and sintered at 450 °C. Average film thicknesses were 7 μm. The films were treated with $TiCl_4$ at 70 °C for 40 min, shown to improve charge separation and collection.[8,9] Some of the cells were sprayed with a TiO_2 blocking underlayer on the FTO before applying the porous film (however, this was found not to influence the results as shown in previous cases of I_3^-/I^-[1,10] and will not be discussed further).

Electrodes were then sensitized by overnight immersion in solutions prepared from sensitizer dyes. Two of the dyes were the well-known ruthenium(II)-based N719 and Z907 prepared in (0.3 mM) solutions of a 1:1 mixture of acetonitrile (ACN) and *tert*-butyl alcohol (TBA). Another set was prepared from the organic, squaraine dye VG5, a new sensitizer with an enhanced absorption in the near-infrared (NIR; strong absorption at 780 nm) to better match the solar emission spectrum.[11]

Transparent counter electrodes were platinized, and the complementary electrode pairs were sealed together with a transparent film of Surlyn at 120 °C. The electrolyte was introduced by injecting 2.5 μL into predrilled holes in the counter electrode. More complete equilibration of the TiO_2 surface to the electrolyte composition was achieved by two additional cycles of removing the electrolyte by vacuum and reinjecting fresh electrolyte, followed by sealing of the holes. We have previously found that interaction of the small volume of electrolyte with the large surface area of the TiO_2 can perturb the electrolyte composition.[12,13]

Received: May 25, 2012
Accepted: July 10, 2012
Published: July 10, 2012

   dx.doi.org/10.1021/jz3006755 | *J. Phys. Chem. Lett.* 2012, 3, 1980−1984

Table 1. Details of Cells Used[a]

electrolyte name	TiO_2	$d/\mu m$	dye	solvent	additives/M			$[I_2]_0$/mM	$[I^-]_0$/mM
Figure 1 N719 iodine series	18NRT Dyesol	7.07	N719	MPN	0.3 TBP, 0.05 GuSCN	PMII	PMITFSI	50	1000; 700; 400; 100
Figure 2 N719 tri-iodide series	18NRT Dyesol	6.81	N719	MPN	0.3 TBP, 0.05 GuSCN	PMII	PMITFSI	136.6; 90.9; 45.4; 22.7; 9.1	1500; 1000; 500; 250; 100
Figure 3 Z907 iodine series	18NRT Dyesol	8.11	Z907	MPN	0.3 TBP, 0.05 GuSCN	PMII	PMITFSI	50	1125; 819; 638; 200
Figure 4 PC iodide series	18NRT Dyesol	~9	N719	PC	0.3 BZI, 0.05 GuSCN	PMII	PMITFSI	50	700; 350; 88; 44
Figure 5 VG5 iodine series	18NRT Dyesol	~7	VG5	MPN		LiI	$LiClO_4$	10	296; 132;88;59;39

[a] d is TiO_2 film thickness. $[I_2]_0$ and $[I^-]_0$ are the initial concentrations of iodine and iodide added to the electrolyte, respectively. MPN: 3-methoxypropionitrile; PC: propylene carbonate; PMII: 1-methyl-3-propylimidazolium iodide; PMITFSI: 1-methyl-3-propylimidazolium bis(trifluoromethylsulfonyl)imide; GuSCN: guanidinium thiocyanate; TBP: *tert*-butylpyridine; BZI: benzimidazole; N719: *cis*-diisothiocyanato-bis(2,2′-bipyridyl-4,4′-dicarboxylato)ruthenium(II) bis(tetrabutylammonium); Z907: *cis*-bis(isothiocyanato)(2,2′-bipyridyl-4,4′-dicarboxylato)(4,4′-dinonyl-2′-bipyridyl)ruthenium(II); VG5:(E)-2-((E)-(5-carboxy-3,3-dimethyl-1-octylindolin-2-ylidene)methyl)-4-((1-ethylbenzo[cd]indol-2-il)-methylene)-3-oxociclobut-1-enolate.

In this paper, five different sets of electrolytes were measured. One set (the "triiodide series") had a variable triiodide concentration, $[I_3^-]_{eq}$, while holding constant the free iodine, $[I_2]_{free}$, i.e., the iodine not bound in the I_3^- complex. A further four different sets (the "iodine series") had a variation in the concentration of $[I_2]_{free}$ with constant $[I_3^-]_{eq}$. To achieve constant free iodine with changing triiodide, the added iodide and iodine concentration were calculated from the known equilibrium of $[I^-]_{eq}$, $[I_2]_{free}$, and $[I_3^-]_{eq}$ (eqs 1 and 2)

$$I_2 + I^- \overset{K_{eq}}{\longleftrightarrow} I_3^- \tag{1}$$

$$K_{eq} = \frac{[I_3^-]_{eq}}{([I^-]_0 - [I_3^-]_{eq})([I_2]_0 - [I_3^-]_{eq})} \tag{2}$$

where $[I^-]_0$ and $[I_2]_0$ are the added iodide and iodine concentrations, and we used $K_{eq} = 10^{6.6}$ in 3-methoxypropionitrile (MPN) and propylene carbonate (PC).[14,15]

In DSSC electrolytes $[I^-]_0$ is always in excess, thus the high binding coefficient, K_{eq}, shifts reaction 1 to the right. Consequently, virtually all the iodine is converted to triiodide.

From eq 2 it can be seen that as long as iodide is in considerable excess, then a constant iodide/added iodine ratio will maintain a constant free iodine concentration $[I_2]_{free}$ (= $[I_2]_0 - [I_3^-]_{eq}$) while varying the triiodide. For the triiodide series, we arbitrarily choose an 11:1 ratio of $[I^-]_0$ to added $[I_2]_0$. Using $K_{eq} = 10^{6.6}$ gave a constant free iodine concentration $[I_2]_{free}$ of 25 nM in all the triiodide cells. Substituting into eq 2, a series of $[I^-]_0$ and added $[I_2]_0$ concentrations were found that would vary $[I_3^-]_{eq}$ while maintianing $[I_2]_{free}$ = 25 nM. This concentration of $[I_2]_{free}$ is similar to the free iodine in normal DSSCs where the iodide/added iodine ratios vary from ~5 to 15.

For the "iodine series", since virtually all the iodine is converted to triiodide, a fixed value of $[I_2]_0$ gives a fixed value of $[I_3^-]_{eq}$, which we wanted to hold constant in this case. We selected a range of $[I^-]_0$ values at fixed $[I_2]_0$ (= 50 mM) and solved eq 2 in full for the exact values of $[I_3^-]_{eq}$ and thus $[I_2]_{free}$.

In our electrolytes, the I^- species was provided by LiI for the VG5 series and PMII for the other remaining series. The total ionic strength across an electrolyte series was maintained at a constant value by substituting with a corresponding concentration of $LiClO_4$ or PMITFSI, respectively. The four sets in the "iodide series" were made from the three dyes and two different solvents, MPN and PC. Additives included guanidinium thiocyanate (GuSCN), and either *tert*-butylpyridine (TBP) or benzimidazole (BZI), typical of a standard working DSSC. The composition and concentrations of each electrolyte are summarized in Table 1.

Measurements. Recombination was measured on complete DSSCs using standard procedures.[16,17] In brief, electron lifetime was measured at V_{OC} over a range of V_{OC}'s by varying light intensity. Electron density in the TiO_2 was also measured for each V_{OC}. The DSSCs were illuminated from the sensitized electrode side by an array of white LEDs (10 W "Solarc" lamps) that provided the bias light for V_{OC} variation. Pump pulses up to 100 μs were generated by an array of 1 W red LEDs controlled by a fast solid state switch. The pulses create a small potential perturbation for V_{OC} decay measurements that were recorded with a National Instruments digital acquisition card. The resulting photovoltage decays were single exponentials and electron lifetimes, τ_n, were extracted by curve fitting.

The concentration of charge stored, Q (C/cm^2), within the TiO_2 was measured using the charge extraction technique.[18,19] The charge density was found using eq 3

$$n = \frac{Q}{qd(1-\theta)} \tag{3}$$

where q is the elementary charge, θ is the porosity, and d is the thickness of the TiO_2 film.

The charge density versus Fermi level in TiO_2 for the "N719 iodine" series in MPN are shown in Figure 1. The Fermi levels are adjusted for shifts in zero potential of each electrolyte

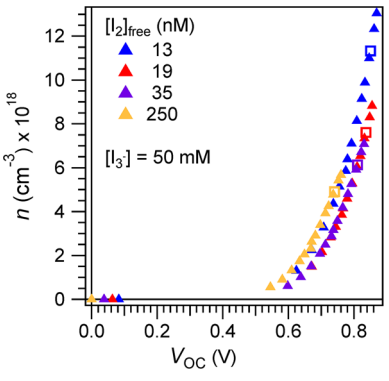

Figure 1. N719 "iodine" series in MPN. Charge density vs Fermi level in TiO_2. V_{OC}'s at 1 sun are highlighted by squares for each electrolyte.

dx.doi.org/10.1021/jz3006755 | J. Phys. Chem. Lett. 2012, 3, 1980−1984

(original data in Figure S1 of the Supporting Information). As usual, charge density increases exponentially with V_{OC}, attributed to an exponential distribution of localized trapping states below the conduction band edge. We make the normal assumption that shifts in charge density as a function of V_{OC} are due to shifts in the conduction band potential relative to the redox potential. This assumption is quantitatively accurate as long as no changes in trap density have occurred. In most of the data presented here, this assumption is supported by the charge extraction data at short circuit plotted as a function of J_{SC} (found in the Supporting Information) as discussed by O'Regan et al.[20] For any exceptions, adjustments to the charge extraction data to account for changes in trap density made no changes to the general trend observed in our results.

Electron lifetimes versus charge density in the TiO_2 from the "N719 iodine" and "N719 triiodide" series are shown in Figure 2a,b, respectively. Overall, both sets show the expected decrease in lifetime, τ_n, with increasing electron density.

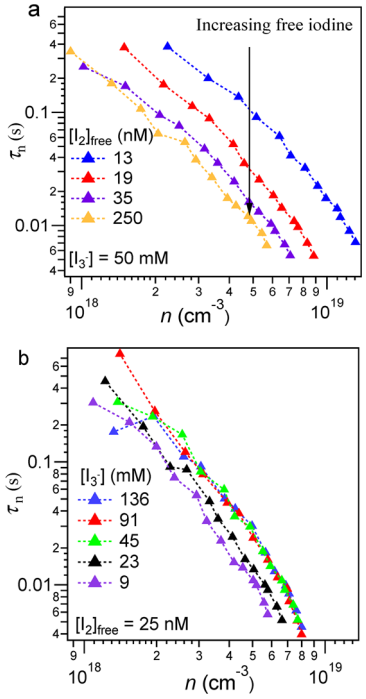

Figure 2. Electron lifetime vs charge density for (a) the N719 "iodine series" and (b) the N719 "triiodide series" in MPN.

For the "N719 iodine" series (Figure 2a), the recombination lifetime decreases strongly with increasing $[I_2]_{free}$ concentration at fixed charge density. The decrease in lifetime is approximately inversely proportional to $[I_2]_{free}$ concentration. For example, a factor of 10 increase of free iodine concentration in the cell reduces the recombination lifetime by a corresponding factor of ~12.

On the other hand, no correlation between τ_n and $[I_3^-]_{eq}$ is observed in Figure 2b for the "triiodide series" where $[I_3^-]_{eq}$ is varied at constant $[I_2]_{free}$. Indeed, the shortest lifetimes, and hence fastest recombination times, are found in cells with the lowest $[I_3^-]_{eq}$. If I_3^- was the primary recombination center, we would expect greater than a 10-fold change in the opposite direction. Another identical "triiodide series" was made and measured that confirmed that τ_n was independent of $[I_3^-]_{eq}$ (see Figure S3a in the Supporting Information).

The observed trends in Figure 2 suggest that the majority of TiO_2 electron−electrolyte recombination occurs via the direct reduction of iodine and not the reduction of triiodide. To determine the generality of this result, we measured the recombination lifetime versus $[I_2]_{free}$ for three additional cell configurations, Z907 in MPN, N719 in PC, and VG5 in MPN, as outlined in Table 1.

Each series in figure 3 again shows faster recombination times with increasing free iodine concentration at constant

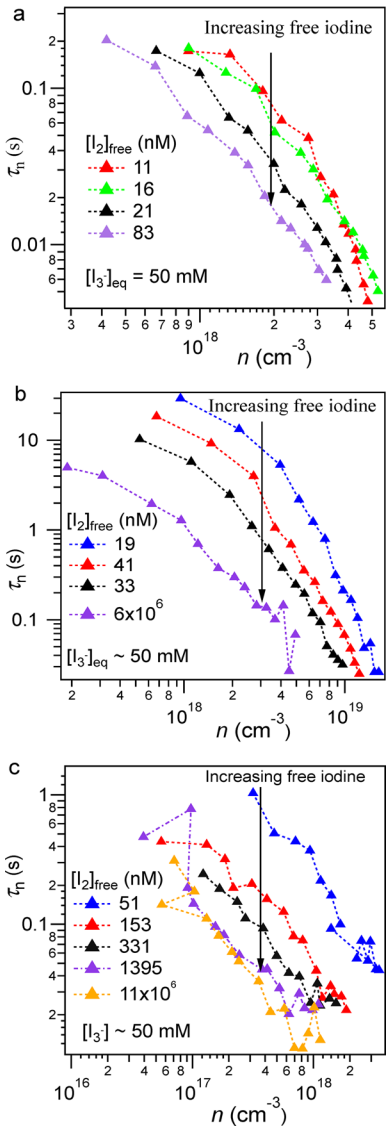

Figure 3. Electron lifetime vs charge density for various free iodine concentrations at constant triiodide concentration for the (a) Z907 "iodine" series in MPN, (b) N719 "iodine" series in PC, and (c) VG5 "iodine" series in MPN.

triodide concentration. The general trend verifies that recombination predominantly occurs via reduction of I_2, even though unbound I_2 is present at much smaller concentrations in the electrolyte.

Although seemingly counterintuitive, the observed trend can be rationalized by plausible differences in the activation barriers of the two reduction mechanisms. For example, if the activation barrier to the reduction of $[I_3^-]_{eq}$ is just 420 meV (40 kJ/mol) higher than that for $[I_2]_{free}$, then the rate constant for $[I_3^-]_{eq}$

dx.doi.org/10.1021/jz3006755 | J. Phys. Chem. Lett. 2012, 3, 1980−1984

would be 7 orders of magnitude slower (ignoring pre-exponential factors). This difference would more than overcome the ~6 orders of magnitude difference in concentration in the standard electrolyte. We note that the activation energy of the reduction of $[I_3^-]_{eq}$ includes the electrostatic energy required to bring the negatively charged $[I_3^-]_{eq}$ close to the electron at the surface.

Two possible confounding factors that might have been present in the data will now be discussed. One of these is the effect of recombination to the photo-oxidized dye (S^+). It is known that the short circuit photocurrent from N719 with 0.1 M iodide is ~20% lower than the photocurrent at higher iodide concentrations due to the reduced rate of regeneration of the dye.[12] This raises the question of whether the recombination lifetimes measured at V_{OC} could contain significant contribution from recombination to S^+ at lower $[I^-]$, as suggested in ref 21. We conclude that they do not for the following reasons. First, the fraction of recombination that goes to S^+ is strongly dependent on light intensity. This is because at lower light intensity the $[S^+]$ decreases, but the concentration of the acceptor in the electrolyte remains unchanged. Quantitatively, the fraction of recombination going to S^+ is given by

$$F_{S+} = k_{rcd}[e^-]^{\gamma}[S^+]/J_{rec} = k_{rcd}[e^-]^{\gamma}/(k_{rcd}[e^-]^{\gamma} + k_{rg}[I^-]) \quad (4)$$

where J_{rec} is the total recombination flux, k_{rcd} is the rate constant for electron−S^+ recombination, and k_{rg} is the rate constant for regeneration of the dye (see Supporting Information). Thus, if F_{S+} was 0.5 at 1 sun, it would be 0.17 at 10% sun, and 0.03 at 1% sun. This is based on the measured relation of $[e^-]$ with intensity, and the measured γ for the cells in Figure 2a (Supporting Information). Given that the trends in recombination lifetime shown in Figures 2 and 3 are almost independent of light intensity over a 50-fold range in light intensity, we can assert that these trends are not related to recombination to the photo-oxidized dye. An exception might be the data for 0.1 M iodide in Figure 2a (250 nM iodine), but the conclusion remains unchanged even with the data. We have also made transient optical measurements to estimate F_{S+} directly (Supporting Information). We find for the 35 nM cell in Figure 2a (0.4 M iodide), the recombination fraction $F_{S+} \lesssim 20\%$.

The other possible issue concerns the impact of the flux of dye regeneration (creating I_3^-) and recombination on the local I_3^- and I_2 concentrations. Overall, these processes have to be balanced at V_{OC}, thus the maximum perturbation in acceptor concentration is equivalent to the number of electrons stored in the TiO_2. For the highest charge density in Figure 1, the perturbation in the acceptor concentration is about 10%[22] (Supporting Information). It might be further asked if the flux dye regeneration might perturb the local I_3^- vs I_2 equilibrium. It so happens that the forward and back reaction rates of eq 1 are very fast, about 10^9 L mol^{-1} sec^{-1} and 10^6 s^{-1}, respectively, in methanol.[23] As a result, the equilibrium is not perturbed at any of the light levels measured here (Supporting Information).

We note that there are several publications that have examined voltage and/or recombination times while changing the amount of iodine added to the electrolyte (e.g., ref 24). As long as iodide is in excess, as it always is, a change in the added iodine changes both the free-iodine and tri-iodide concentration by the same fraction due to the equilibrium in eq 1. Although these publications have not claimed to distinguish recombination to free-iodide from that to tri-iodide, we highlight that this type of data is not useful for our purpose.

In summary, we have carried out charge extraction and transient photovoltage measurements on DSSCs to correlate the recombination kinetics with a concentration variation in either the free iodine or triiodide acceptor species in the electrolyte. All measurements showed that at a fixed charge density the recombination lifetime τ_n decreases with increasing $[I_2]_{free}$. This trend was observed across four sets of DSSCs made with the dyes N719, Z907, and VG5 in the solvent MPN and one with N719 dye in PC electrolyte solvent. No correlation was found between τ_n and variation in $[I_3^-]_{eq}$. We conclude that the majority of recombination occurs by direct reduction of iodine in most if not all DSSCs.

■ ASSOCIATED CONTENT

Supporting Information

Charge density versus V_{OC} for the N719 "iodine series" including redox potentials. Charge extraction data at short circuit and charge density versus V_{OC} from another N719 "triiodide" series. Calculations and discusison on the impact of dye regeneration and acceptor perturbation on recombination. This material is available free of charge via the Internet at http://pubs.acs.org.

■ AUTHOR INFORMATION

Corresponding Author

*E-mail: b.oregan@imperial.ac.uk.

Notes

The authors declare no competing financial interest.

■ ACKNOWLEDGMENTS

This work was supported by the UK EPSRC project APEX (EP/H040218/1), and the EU FP7 project SMARTOP (ref#265769). The authors also gratefully acknowledge the funding contribution from the Alan Howard scholarships for Energy Futures.

■ REFERENCES

(1) Boschloo, G.; Hagfeldt, A. Characteristics of the Iodide/Triiodide Redox Mediator in Dye-Sensitized Solar Cells. *Acc. Chem. Res.* **2009**, *42*, 1819−1826.

(2) Koops, S. E.; O'Regan, B. C.; Barnes, P. R. F.; Durrant, J. R. Parameters Influencing the Efficiency of Electron Injection in Dye-Sensitized Solar Cells. *J. Am. Chem. Soc.* **2009**, *131*, 4808−4818.

(3) Peter, L. M. Characterization and Modeling of Dye-Sensitized Solar Cells. *J. Phys. Chem. C* **2007**, *111*, 6601−6612.

(4) Rowley, J.; Meyer, G. J. Reduction of I_2/I_3^- by Titanium Dioxide. *J. Phys. Chem. Lett.* **2009**, *113*, 18444−18447.

(5) Huang, S. Y.; Schlichthorl, G.; Nozik, A. J.; Grätzel, M.; Frank, A. J. Charge Recombination in Dye-Sensitized Nanocrystalline TiO_2 Solar Cells. *J. Phys. Chem. B* **1997**, *101*, 2576−2582.

(6) Yu, Z.; Gorlov, M.; Nissfolk, J.; Boschloo, G.; Kloo, L. Investigation of Iodine Concentration Effects in Electrolytes for Dye-Sensitized Solar Cells. *J. Phys. Chem. C* **2010**, *114*, 10612−10620.

(7) Barnes, P. R. F.; Anderson, A. Y.; Koops, S. E.; Durrant, J. R.; O'Regan, B. C. Electron Injection Efficiency and Diffusion Length in Dye-Sensitized Solar Cells Derived from Incident Photon Conversion Efficiency Measurements. *J. Phys. Chem. C* **2009**, *113*, 1126−1136.

(8) O'Regan, B. C.; Durrant, J. R.; Sommeling, P. M.; Bakker, N. J. Influence of the $TiCl_4$ Treatment on Nanocrystalline TiO_2 Films in Dye-Sensitized Solar Cells. 2. Charge Density, Band Edge Shifts, and Quantification of Recombination Losses at Short Circuit. *J. Phys. Chem. C* **2007**, *111*, 14001−14010.

(9) Ito, S.; Liska, P.; Comte, P.; Charvet, R.; Péchy, P.; Bach, U.; Schmidt-Mende, L.; Zakeeruddin, S. M.; Kay, A.; Nazeeruddin, M. K.; et al. Control of Dark Current in Photoelectrochemical (TiO_2/I^- − I_3^-) and Dye-Sensitized Solar Cells. *Chem. Commun.* **2005**, 4351−4353.
(10) Cameron, P. J.; Peter, L. M. How Does Back-Reaction at the Conducting Glass Substrate Influence the Dynamic Photovoltage Response of Nanocrystalline Dye-Sensitized Solar Cells? *J. Phys. Chem. B* **2005**, *109*, 7392−7398.
(11) Martiniani, S.; Anderson, A. Y.; Law, C.; O'Regan, B. C.; Barolo, C. New Insight into the Regeneration Kinetics of Organic Dye Sensitised Solar Cells. *Chem. Commun.* **2012**, *48*, 2406−2408.
(12) Anderson, A. Y.; Barnes, P. R. F.; Durrant, J. R.; O'Regan, B. C. Quantifying Regeneration in Dye-Sensitized Solar Cells. *J. Phys. Chem. C* **2011**, *115*, 2439−2447.
(13) Miettunen, K.; Asghar, I.; Mastroianni, S.; Halmea, J.; Barnes, P. R. F.; Rikkinen, E.; O'Regan, B. C.; Lund, P. Effect of Molecular Filtering and Electrolyte Composition on the Spatial Variation in Performance of Dye Solar Cells. *J. Electroanal. Chem.* **2012**, *663*, 63−72.
(14) Nelson, I. V.; Iwamoto, R. T. Voltammetric Evaluation of the Stability of Trichloride, Tribromide, and Triiodide Ions in Nitromethane, Acetone, and Acetonitrile. *J. Electroanal. Chem.* **1963**, *7*, 218−221.
(15) Ue, M.; Takeda, M.; Takehara, M.; Mori, S. Electrochemical Properties of Quaternary Ammonium Salts for Electrochemical Capacitors. *J. Electrochem. Soc.* **1997**, *144*, 2684−2688.
(16) O'Regan, B. C.; Bakker, K.; Kroeze, J.; Smit, H.; Sommeling, P.; Durrant, J. R. Measuring Charge Transport from Transient Photovoltage Rise Times. A New Tool To Investigate Electron Transport in Nanoparticle Films. *J. Phys. Chem. B* **2006**, *110*, 17155−17160.
(17) O'Regan, B. C.; Durrant, J. R. Kinetic and Energetic Paradigms for Dye-Sensitized Solar Cells: Moving from the Ideal to the Real. *Acc. Chem. Res.* **2009**, *42*, 1799−1808.
(18) Duffy, N. W.; Peter, L. M.; Rajapakse, R. M. G.; Wijayantha, K. G. U. A Novel Charge Extraction Method for the Study of Electron Transport and Interfacial Transfer in Dye Sensitised Nanocrystalline Solar Cells. *Electrochem. Commun.* **2000**, *2*, 658−662.
(19) Barnes, P. R. F.; Anderson, A. Y.; Juozapavicius, M.; Liu, L.; Li, X.; Palomares, E.; Forneli, A.; O'Regan, B. C. Factors Controlling Charge Recombination under Dark and Light Conditions in Dye Sensitised Solar Cells. *Phys. Chem. Chem. Phys.* **2011**, *113*, 3547−3558.
(20) O'Regan, B.; Li, X.; Ghaddar, T. Dye Adsorption, Desorption, and Distribution in Mesoporous TiO_2 Films, and Its Effects on Recombination Losses in Dye Sensitized Solar Cells. *Energy Environ. Sci.* **2012**, *5*, 7203−7215.
(21) Miyashita, M.; Sunahara, K.; Nishikawa, T.; Uemura, Y.; Koumura, N.; Hara, K.; Mori, A.; Abe, T.; Suzuki, E.; Mori, S. Interfacial Electron-Transfer Kinetics in Metal-Free Organic Dye-Sensitized Solar Cells: Combined Effects of Molecular Structure of Dye and Electrolytes. *J. Am. Chem. Soc.* **2008**, *130*, 17874−17881.
(22) Barnes, P. R. F.; Anderson, A. Y.; Durrant, J. R.; O'Regan, B. C. Simulation and Measurement of Complete Dye Sensitised Solar Cells: Including the Influence of Trapping, Electrolyte, Oxidised Dyes and Light Intensity on Steady State and Transient Device Behaviour. *Phys. Chem. Chem. Phys.* **2011**, *13*, 5798−5816.
(23) Ruasse, M. F.; Aubard, J.; Galland, B.; Adenier, A. Kinetic Study of the Fast Halogen−Trihalide Ion Equilibria in Protic Media by the Raman-Laser Temperature-Jump Technique. A Non-Diffusion-Controlled Ion−Molecule Reaction. *J. Phys. Chem. B* **1986**, *90*, 4382−4388.
(24) Bisquert, J.; Zaban, A.; Greenshtein, M.; Mora-Seró, I. Determination of Rate Constants for Charge Transfer and the Distribution of Semiconductor and Electrolyte Electronic Energy Levels in Dye-Sensitized Solar Cells by Open-Circuit Photovoltage Decay Method. *J. Am. Chem. Soc.* **2004**, *126*, 13550−13559.